Negative phase velocity in a uniformly moving, homogeneous, isotropic, dielectric-magnetic medium

2004 J. Phys. A: Math. Gen. 37 5697

(http://iopscience.iop.org/0305-4470/37/21/015)

INSTITUTE OF PHYSICS PUBLISHING JOURNAL OF PHYSICS A: MATHEMATICAL AND GENERAL

J. Phys. A: Math. Gen. **37** (2004) 5697–5711 PII: S0305-4470(04)74365-6

Negative phase velocity in a uniformly moving, homogeneous, isotropic, dielectric-magnetic medium

Tom G Mackay[1] **and Akhlesh Lakhtakia**[2]

[1] School of Mathematics, University of Edinburgh, Edinburgh EH9 3JZ, UK
[2] CATMAS—Computational and Theoretical Materials Sciences Group, Department of Engineering Science and Mechanics, Pennsylvania State University, University Park, PA 16802-6812, USA

E-mail: T.Mackay@ed.ac.uk

Received 8 January 2004, in final form 17 March 2004
Published 12 May 2004
Online at stacks.iop.org/JPhysA/37/5697
DOI: 10.1088/0305-4470/37/21/015

Abstract
Homogeneous, isotropic mediums characterized by relative permittivity scalars $\epsilon = \epsilon_R + i\epsilon_I$ ($\epsilon_R, \epsilon_I \in \mathbb{R}$) and relative permeability scalars $\mu = \mu_R + i\mu_I$ ($\mu_R, \mu_I \in \mathbb{R}$) are well known to support the propagation of plane waves with negative phase velocity (NPV), provided that both $\epsilon_R < 0$ and $\mu_R < 0$. We demonstrate that mediums which do not support NPV propagation when viewed at rest (e.g., mediums with $\epsilon_R > 0$ and $\mu_R > 0$), can support NPV propagation when they are viewed in a reference frame which is uniformly translated at a sufficiently high velocity. Representative numerical examples are used to explore the constitutive parameter regimes which support NPV propagation under the uniform-velocity condition.

PACS numbers: 03.30.+p, 03.50.De

1. Introduction

In the late 1960s, Veselago speculated upon the properties of a homogeneous, lossless, isotropic dielectric-magnetic medium with relative permittivity scalar $\epsilon < 0$ and relative permeability scalar $\mu < 0$ [1, 2]. A range of exotic and potentially useful phenomenons—such as negative refraction, negative Doppler shift and inverse Čerenkov radiation—were predicted for mediums of this type. After a lapse of 30 years, interest in these types of mediums was rekindled, following experimental evidence of their existence in the form of microwave metamaterials [3, 4]. Subsequent experimental [5, 6] and theoretical [7–9] studies have confirmed Veselago's original thesis; see [10] for an up-to-date review.

A central characteristic of mediums with $\epsilon < 0$ and $\mu < 0$ is that they support the propagation of plane waves with the phase-velocity vector directed opposite to the time-averaged Poynting vector. Accordingly, we describe such mediums as *negative phase-velocity*

(NPV) mediums, in contrast to conventional *positive phase-velocity* (PPV) mediums in which the phase velocity has the same direction as the power flow.

Although $\epsilon < 0$ and $\mu < 0$ is a sufficient condition for NPV propagation, it is not a necessary condition. In fact, for dissipative isotropic dielectric–magnetic mediums with complex-valued $\epsilon = \epsilon_R + \mathrm{i}\epsilon_I$ ($\epsilon_R, \epsilon_I \in \mathbb{R}$) and complex-valued $\mu = \mu_R + \mathrm{i}\mu_I$ ($\mu_R, \mu_I \in \mathbb{R}$), it is sufficient for only one of ϵ_R or μ_R to be negative for NPV propagation to develop [11]. The restrictions on the signs of the constitutive parameters may be further reduced by considering anisotropic mediums [12–14].

The following question arises naturally in the present context: Can a medium which is of the PPV type when viewed in a stationary reference frame be of the NPV type when viewed in a reference frame moving at constant velocity? A glimpse of the answer to this question can be found in many textbook treatments of electromagnetic fields in uniformly moving mediums; see [15], for example. But in those treatments, it is assumed that the moving substance has purely instantaneous response and is therefore nondissipative; such mediums are not causal. We, however, address the question comprehensively for dissipative mediums in the following sections.

A note on notation: ϵ_0 and μ_0 are the permittivity and the permeability of free space (i.e. vacuum), respectively; $c_0 = (\epsilon_0\mu_0)^{-1/2}$ is the speed of light in free space; ω is the angular frequency; $\hat{\mathbf{v}}$ is a unit vector co-directional with $\mathbf{v}$; the unit dyadic is $\underline{\underline{I}}$ and $\mathbf{r}$ denotes the spatial coordinate vector.

2. Analysis

2.1. Minkowski constitutive relations

Suppose an inertial reference frame Σ' moves with a constant velocity $\mathbf{v} = v\hat{\mathbf{v}}$ with respect to an inertial reference frame Σ. By virtue of the Lorentz covariance of the Maxwell postulates, the electromagnetic field phasors in frame Σ are related as

$$\left.\begin{aligned} \nabla \times \mathbf{E} - \mathrm{i}\omega\mathbf{B} = \mathbf{0} \\ \nabla \times \mathbf{H} + \mathrm{i}\omega\mathbf{D} = \mathbf{0} \end{aligned}\right\} \tag{1}$$

and the electromagnetic field phasors in frame Σ' are related as

$$\left.\begin{aligned} \nabla' \times \mathbf{E}' - \mathrm{i}\omega'\mathbf{B}' = \mathbf{0} \\ \nabla' \times \mathbf{H}' + \mathrm{i}\omega'\mathbf{D}' = \mathbf{0} \end{aligned}\right\}. \tag{2}$$

The relationships between the primed and unprimed phasors in (1) and (2) are provided via the Lorentz transformation as [15]

$$\mathbf{E}' = (\mathbf{E}\cdot\hat{\mathbf{v}})\hat{\mathbf{v}} + \frac{1}{\sqrt{1-\beta^2}}[(\underline{\underline{I}} - \hat{\mathbf{v}}\hat{\mathbf{v}})\cdot\mathbf{E} + \mathbf{v}\times\mathbf{B}] \tag{3}$$

$$\mathbf{B}' = (\mathbf{B}\cdot\hat{\mathbf{v}})\hat{\mathbf{v}} + \frac{1}{\sqrt{1-\beta^2}}\left[\left(\underline{\underline{I}} - \hat{\mathbf{v}}\hat{\mathbf{v}}\right)\cdot\mathbf{B} - \frac{\mathbf{v}\times\mathbf{E}}{c_0^2}\right] \tag{4}$$

$$\mathbf{H}' = (\mathbf{H}\cdot\hat{\mathbf{v}})\hat{\mathbf{v}} + \frac{1}{\sqrt{1-\beta^2}}[(\underline{\underline{I}} - \hat{\mathbf{v}}\hat{\mathbf{v}})\cdot\mathbf{H} - \mathbf{v}\times\mathbf{D}] \tag{5}$$

$$\mathbf{D}' = (\mathbf{D}\cdot\hat{\mathbf{v}})\hat{\mathbf{v}} + \frac{1}{\sqrt{1-\beta^2}}\left[\left(\underline{\underline{I}} - \hat{\mathbf{v}}\hat{\mathbf{v}}\right)\cdot\mathbf{D} + \frac{\mathbf{v}\times\mathbf{H}}{c_0^2}\right] \tag{6}$$

where $\beta = v/c_0$.

Let us now consider a homogeneous, isotropic, dielectric-magnetic medium which is stationary in the reference frame Σ'; its constitutive relations may be expressed as

$$\left.\begin{aligned} \mathbf{D}' &= \epsilon_0\epsilon\mathbf{E}' = \epsilon_0(\epsilon_R + \mathrm{i}\epsilon_I)\mathbf{E}' \\ \mathbf{B}' &= \mu_0\mu\mathbf{B}' = \mu_0(\mu_R + \mathrm{i}\mu_I)\mathbf{B}'. \end{aligned}\right\} \tag{7}$$

Substituting the transformation equations (3)–(6) into (7) leads to the Minkowski constitutive relations of the dielectric–magnetic medium in the reference frame Σ [15], namely

$$\left.\begin{aligned} \mathbf{D} &= \epsilon_0\epsilon\underline{\underline{\alpha}}\cdot\mathbf{E} + \frac{m\hat{\mathbf{v}}\times\mathbf{H}}{c_0} \\ \mathbf{B} &= -\frac{m\hat{\mathbf{v}}\times\mathbf{E}}{c_0} + \mu_0\mu\underline{\underline{\alpha}}\cdot\mathbf{H} \end{aligned}\right\} \tag{8}$$

wherein

$$\underline{\underline{\alpha}} = \alpha\underline{\underline{I}} + (1-\alpha)\hat{\mathbf{v}}\hat{\mathbf{v}} \tag{9}$$

$$\alpha = \frac{1-\beta^2}{1-\epsilon\mu\beta^2} \tag{10}$$

$$m = \beta\frac{\epsilon\mu - 1}{1-\epsilon\mu\beta^2}. \tag{11}$$

On setting $v = 0$, the constitutive relations (8) for Σ degenerate to those of Σ' specified in (7).

2.2. *Planewave propagation*

We turn now to the propagation of plane waves with field phasors

$$\left.\begin{aligned} \mathbf{E} &= \mathbf{E}_0\exp(\mathrm{i}\mathbf{k}\cdot\mathbf{r}) \\ \mathbf{H} &= \mathbf{E}_0\exp(\mathrm{i}\mathbf{k}\cdot\mathbf{r}) \end{aligned}\right\} \tag{12}$$

in the medium described by the Minkowski constitutive relations (8). A brief outline of the theory is provided here; for further details the reader is referred elsewhere [15–17].

Combining (12) with the Maxwell curl postulates (1), and utilizing the constitutive relations (8) to eliminate $\mathbf{D}$ and $\mathbf{B}$, we find that planewave solutions satisfy the relation [15]

$$\underline{\underline{W}}\cdot\mathbf{E}_0 = \mathbf{0} \tag{13}$$

where

$$\underline{\underline{W}} = \left[\omega^2\epsilon_0\epsilon\mu_0\mu\det(\underline{\underline{\alpha}}) - \left(\mathbf{k}+\frac{\omega m}{c_0}\hat{\mathbf{v}}\right)\cdot\underline{\underline{\alpha}}\cdot\left(\mathbf{k}+\frac{\omega m}{c_0}\hat{\mathbf{v}}\right)\right]\underline{\underline{I}} + \left(\mathbf{k}+\frac{\omega m}{c_0}\hat{\mathbf{v}}\right)\left(\mathbf{k}+\frac{\omega m}{c_0}\hat{\mathbf{v}}\right)\cdot\underline{\underline{\alpha}}. \tag{14}$$

Without loss of generality, the wave propagation vector $\mathbf{k}$ can be taken along the z axis, while the velocity vector lies in the xz plane; i.e.

$$\left.\begin{aligned} \mathbf{k} &= k\hat{\mathbf{u}}_z = (k_R + \mathrm{i}k_I)\hat{\mathbf{u}}_z \\ \hat{\mathbf{v}} &= \hat{\mathbf{u}}_x\sin\theta + \hat{\mathbf{u}}_z\cos\theta \end{aligned}\right\} \tag{15}$$

where k_R and k_I are the real and imaginary parts of the wavenumber k. Accordingly, the phase velocity is given by

$$\mathbf{v}_{\mathrm{ph}} = \frac{\omega}{k_R}\hat{\mathbf{u}}_z. \tag{16}$$

The dispersion relation

$$\det(\underline{\underline{W}}) = 0 \tag{17}$$

yields the wavenumbers as

$$k = \frac{\omega}{c_0} \frac{-\beta\xi\cos\theta \pm \sqrt{1 + \xi(1 - \beta^2\cos^2\theta)}}{1 - \xi\beta^2\cos^2\theta} \tag{18}$$

with

$$\xi = \frac{\epsilon\mu - 1}{1 - \beta^2}. \tag{19}$$

By selecting the sign of the square root term in (18) to be such that $k_I > 0$, we ensure that the positive z axis is the direction of wave attenuation. Observe that in spite of the Minkowski constitutive relations indicating anisotropy when $v \neq 0$, the medium is unirefringent.

The orthogonality condition

$$\left(\mathbf{k} + m\frac{\omega}{c_0}\hat{\mathbf{v}}\right) \cdot \underline{\underline{\alpha}} \cdot \mathbf{E}_0 = 0 \tag{20}$$

emerges by combining the dispersion relation (17) with (13). In consideration of (20), eigenvector solutions to (13) are provided by linear combinations of the orthogonal pair

$$\mathbf{e}_1 = \mathbf{k} \times \hat{\mathbf{v}} \tag{21}$$

$$\mathbf{e}_2 = \underline{\underline{\alpha}}^{-1} \cdot \left[\left(\mathbf{k} + m\frac{\omega}{c_0}\hat{\mathbf{v}}\right) \times \mathbf{e}_1\right]. \tag{22}$$

Thus, the electric field phasor $\mathbf{E}$ can be set down as [15]

$$\mathbf{E} = (C_1\,\mathbf{e}_1 + C_2\,\mathbf{e}_2)\exp(\mathrm{i}kz) \tag{23}$$

wherein C_1 and C_2 are arbitrary constants. The corresponding magnetic field phasor

$$\mathbf{H} = \left[\frac{C_1}{\omega\mu_0\mu}\,\mathbf{e}_2 - \omega\epsilon_0\epsilon C_2\,\mathbf{e}_1\right]\exp(\mathrm{i}kz) \tag{24}$$

is provided by the Maxwell curl postulates (1) together with (23) and the constitutive relations (8).

2.3. Poynting vector

An expression of the time-averaged Poynting vector can be derived from the definition

$$\mathbf{P} = \tfrac{1}{2}\,\mathrm{Re}(\mathbf{E} \times \mathbf{H}^*) \tag{25}$$

wherein $\mathrm{Re}(\cdot)$ denotes the real part and the asterisk denotes the complex conjugate. For lossless dielectric–magnetic mediums (i.e. those mediums characterized by $\epsilon_I = 0$ and $\mu_I = 0$), we have [15]

$$\mathbf{P} = \frac{\left(|C_1|^2 + \omega^2\epsilon_0\epsilon_R\mu_0\mu_R|C_2|^2\right)(\mathbf{k} \times \hat{\mathbf{v}})^2}{2\omega\mu_0\mu_R}\left[\mathbf{k} + \frac{\xi\,(\omega - \mathbf{k}\cdot\mathbf{v})}{c_0^2}\mathbf{v}\right] \tag{26}$$

but explicit representations for $\mathbf{P}$ are not readily tractable for dissipative mediums. Our particular interest lies in the component of $\mathbf{P}$ parallel to the wavevector, namely $P_z = \hat{\mathbf{u}}_z \cdot \mathbf{P}$, for dissipative mediums. When $C_2 = 0$, we find

$$P_z \sim P_{z1}\exp(-2k_I z) \tag{27}$$

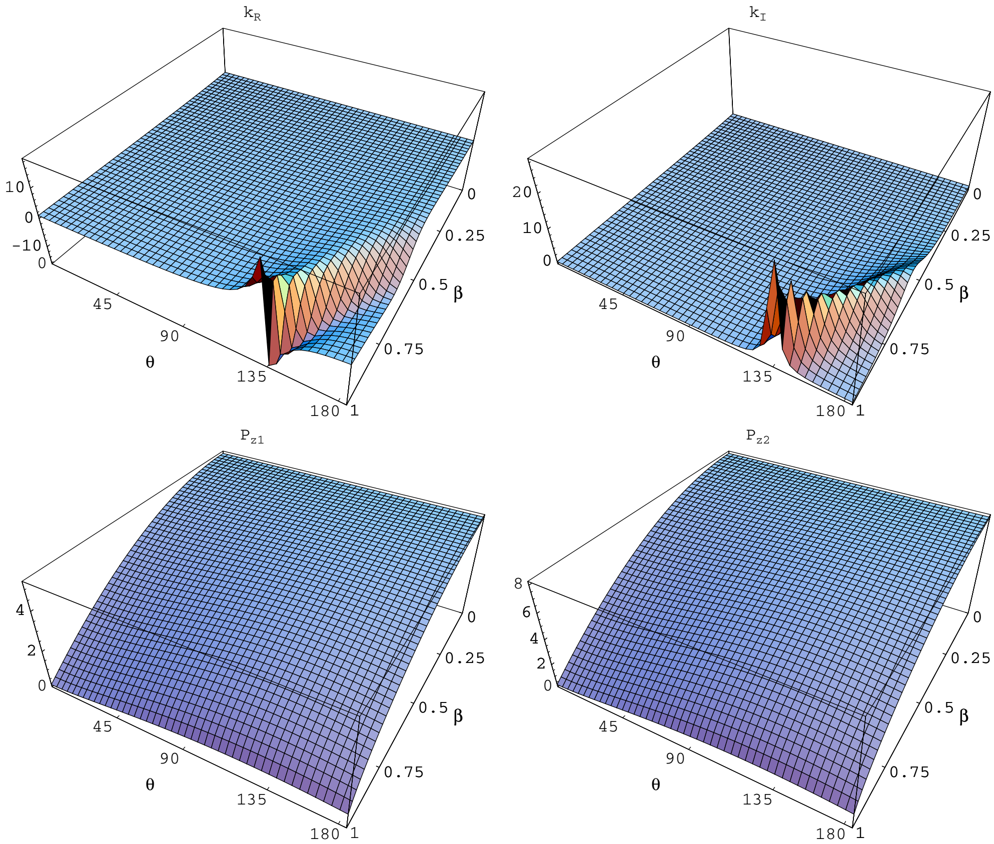

Figure 1. For $\epsilon = 3 + i2\delta$ and $\mu = 2 + i\delta$, the real (k_R) and imaginary (k_I) parts of the wavenumber k (normalized with respect to ω/c_0), along with the associated values of P_{z1} and P_{z2}, plotted against θ (in degrees) and β for $\delta = 0.5$.

with

$$P_{z1} = \left\{ \frac{\omega}{c_0\left(k_R^2 + k_I^2\right)} \left[(k_R\epsilon_R + k_I\epsilon_I)\left(\mu_R^2 + \mu_I^2\right) - (k_R\mu_R - k_I\mu_I)\beta^2\right] - \left[\epsilon_R\left(\mu_R^2 + \mu_I^2\right) - \mu_R\right]\beta\cos\theta \right\} \tag{28}$$

while

$$P_z \sim P_{z2}\exp(-2k_I z) \tag{29}$$

with

$$P_{z2} = \left\{ \frac{\omega}{c_0\left(k_R^2 + k_I^2\right)} \left[(k_R\mu_R + k_I\mu_I)\left(\epsilon_R^2 + \epsilon_I^2\right) - (k_R\epsilon_R - k_I\epsilon_I)\beta^2\right] - \left[\mu_R\left(\epsilon_R^2 + \epsilon_I^2\right) - \epsilon_R\right]\beta\cos\theta \right\} \tag{30}$$

holds when $C_1 = 0$. In view of (23) and (24), it is clear that $P_z > 0$ provided that both $P_{z1} > 0$ and $P_{z2} > 0$.

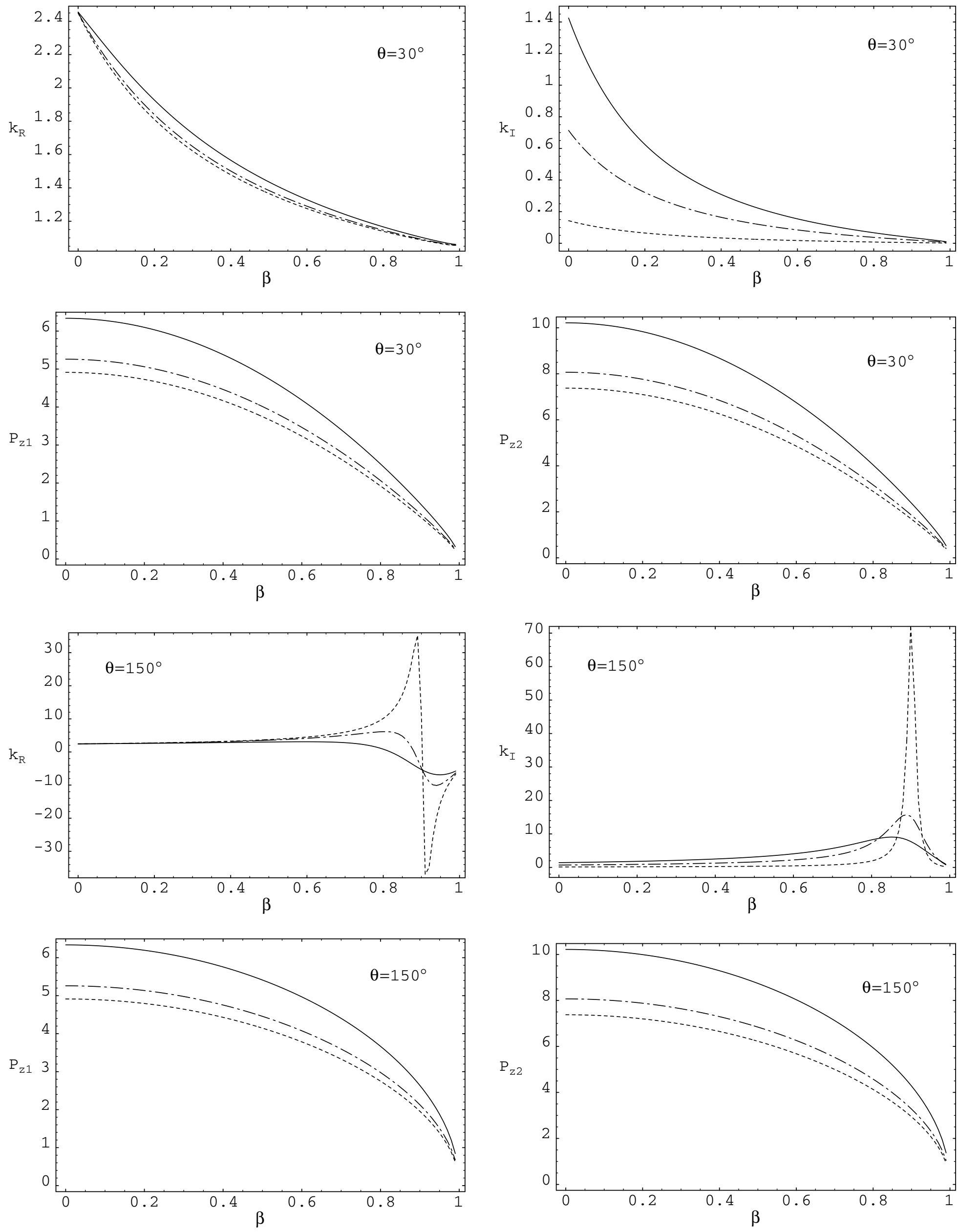

Figure 2. For $\epsilon = 3 + i2\delta$ and $\mu = 2 + i\delta$, the real (k_R) and imaginary (k_I) parts of the wavenumber k (normalized with respect to ω/c_0), along with the associated values of P_{z1} and P_{z2}, plotted against β for $\theta = 30^\circ$ and 150°. Key: the dotted, broken dotted and solid lines denote $\delta = 0.1$, 0.5 and 1, respectively.

3. Numerical results

Let us explore planewave propagation for three scenarios, viz

(a) $\epsilon_R > 0$ and $\mu_R > 0$;

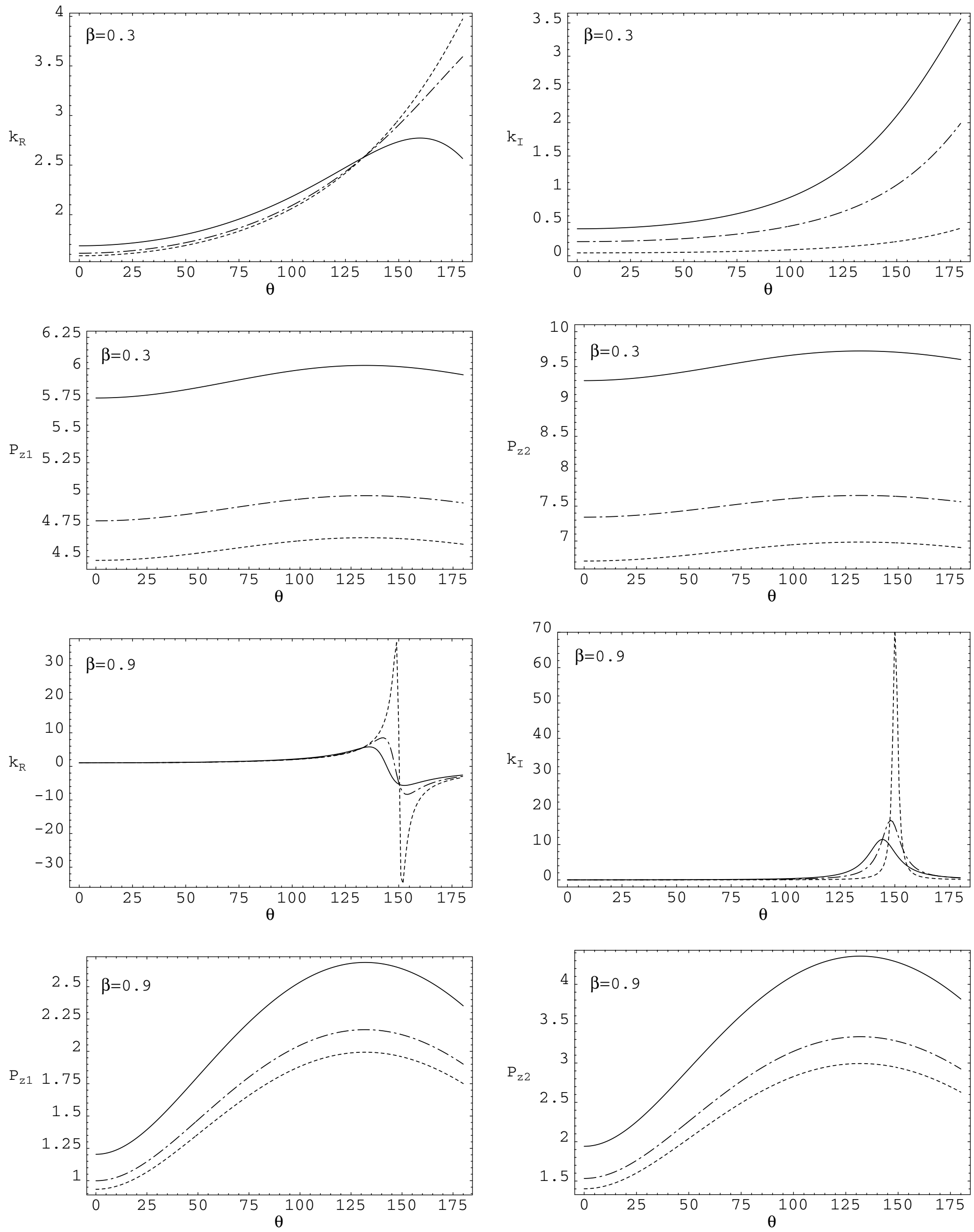

Figure 3. For $\epsilon = 3 + \mathrm{i}2\delta$ and $\mu = 2 + \mathrm{i}\delta$, the real ($k_R$) and imaginary ($k_I$) parts of the wavenumber k (normalized with respect to ω/c_0), along with the associated values of P_{z1} and P_{z2}, plotted against θ (in degrees) for $\beta = 0.3$ and 0.9. Key: as in figure 2.

(b) $\epsilon_R > 0$ and $\mu_R < 0$; and

(c) $\epsilon_R < 0$ and $\mu_R < 0$

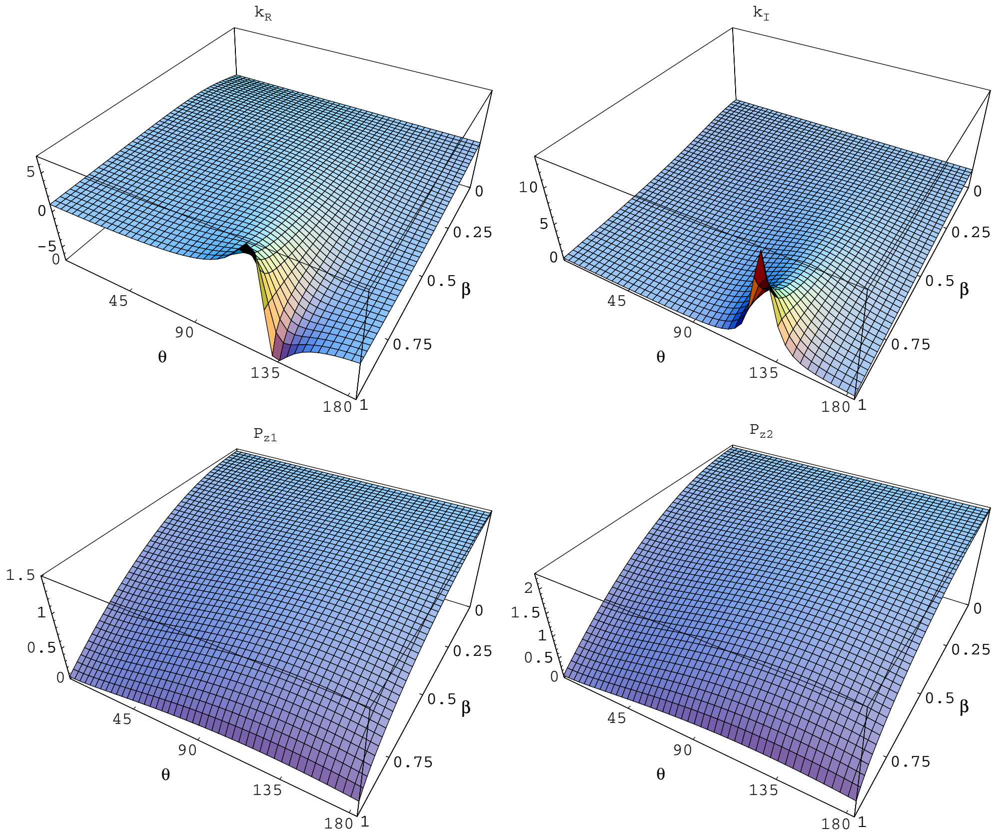

Figure 4. As figure 1 but with $\epsilon = 3 + i2\delta$ and $\mu = -2 + i\delta$.

by means of representative numerical examples. Note that the case $\{\epsilon_R < 0, \mu_R > 0\}$ is complementary to (b) and therefore need not be investigated here. The principle of causality imposes the constraints $\epsilon_I > 0$ and $\mu_I > 0$ on actual materials [18].

Temporal dispersion is accommodated through the implicit dependences of ϵ and μ upon ω. The results presented here are independent of whether the dielectric–magnetic medium exhibits normal temporal dispersion or anomalous temporal dispersion. Accordingly, in interpreting results, we consider the relative orientations of energy flow associated with a plane wave (as provided by the Poynting vector) and the phase velocity, but group velocity (which is the velocity of the peak of a wavepacket) is not discussed [15]. The effects of spatial dispersion are also not considered here.

3.1. $\epsilon_R > 0$ *and* $\mu_R > 0$

For $\epsilon = 3 + i2\delta$ and $\mu = 2 + i\delta$ with $\delta = 0.5$, the real (k_R) and imaginary (k_I) parts of the wavenumber k, together with the associated values of P_{z1} and P_{z2}, are plotted in figure 1 as functions of θ and β. The quantities k_R, k_I, P_{z1} and P_{z2} are >0 across much of the $\theta\beta$ plane. That is, the phase-velocity vector is co-parallel with power flow for most values of θ and β. However, when θ and β are both large, k_R becomes negative while k_I, P_{z1} and P_{z2} remain positive in figure 1. NPV propagation is thereby signified.

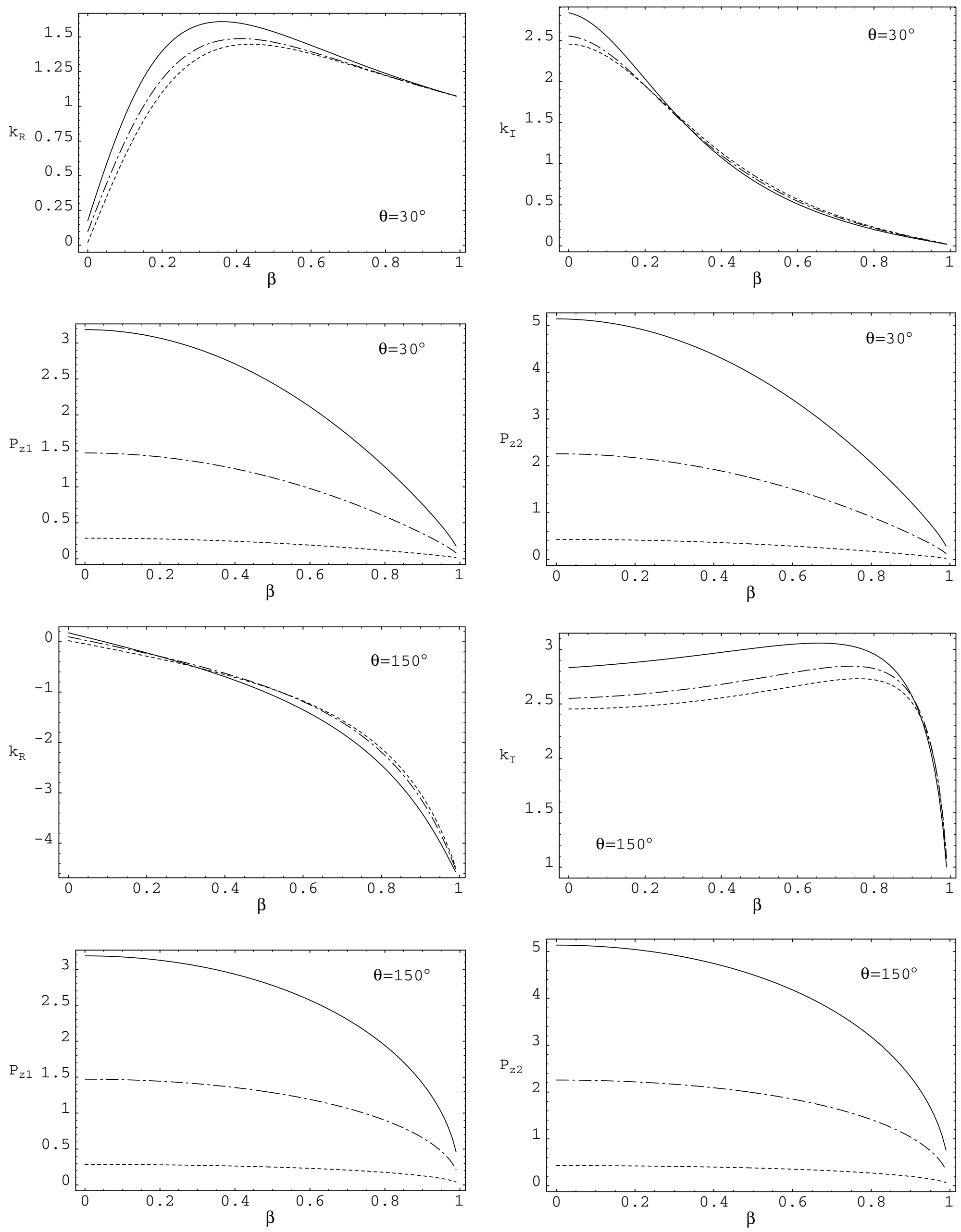

Figure 5. As figure 2 but with $\epsilon = 3 + i2\delta$ and $\mu = -2 + i\delta$.

The transition from positive to negative phase velocity is considered in further detail in figure 2 where k_R, k_I, P_{z1} and P_{z2} are plotted against β for three different values of dissipation parameter δ. At $\theta = \pi/6$, PPV behaviour is observed for all values of $\beta \in (0, 1)$. On the other hand, when $\theta = 5\pi/6$, k_R becomes negative—indicating that the phase velocity is directed opposite to the power flow—for large values of β. The transition from $k_R > 0$ to $k_R < 0$

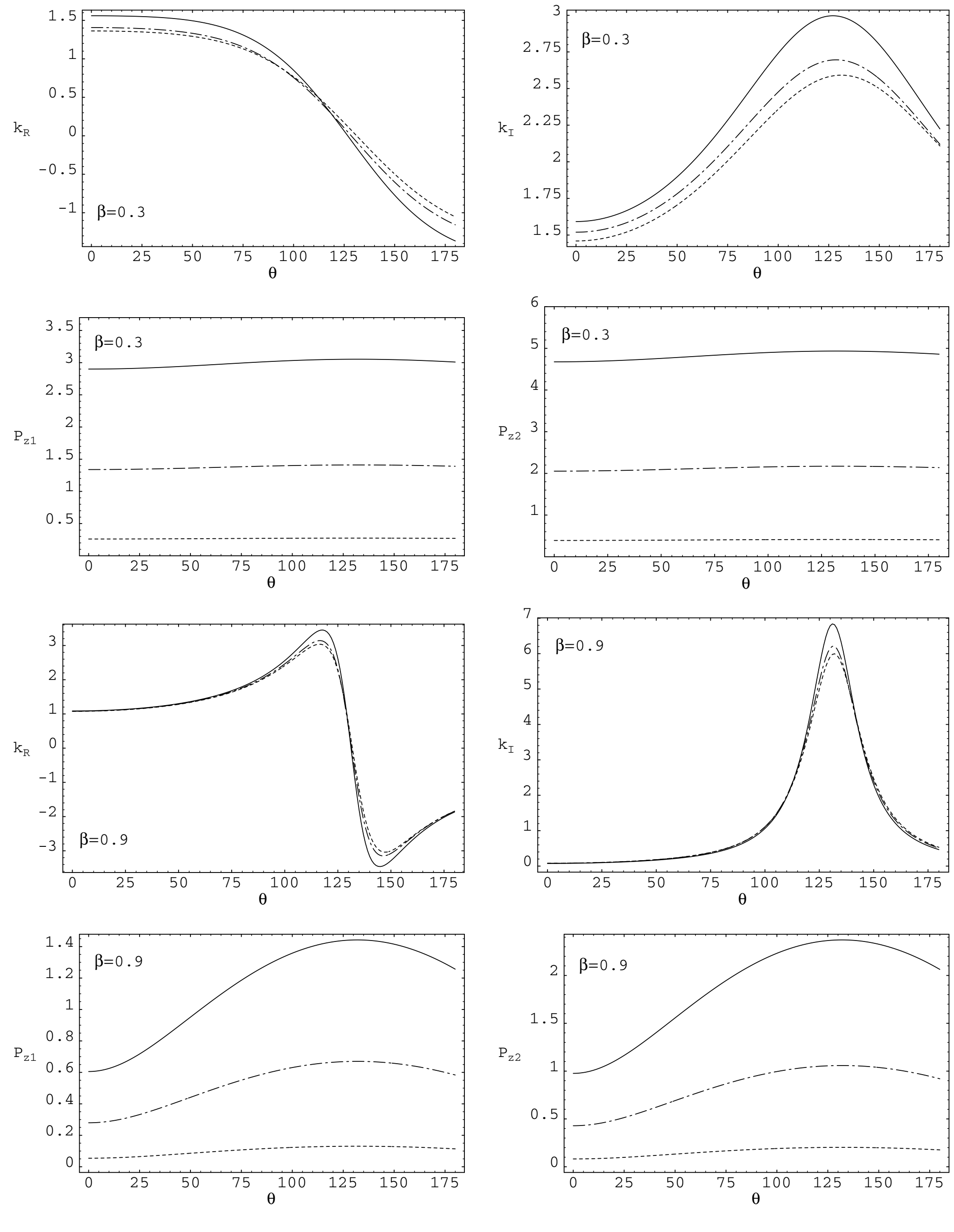

Figure 6. As figure 3 but with $\epsilon = 3 + \mathrm{i}2\delta$ and $\mu = -2 + \mathrm{i}\delta$.

coincides with a local maximum in k_I. This maximum is particularly pronounced at low values of δ.

Similar behaviour is observed when k_R, k_I, P_{z1} and P_{z2} are viewed as functions of θ, as revealed in figure 3. For $\beta = 0.3$, only positive values of k_R are observed for all angles $\theta \in (0, \pi)$. When $\beta = 0.9$, transitions from positive to negative values of k_R,

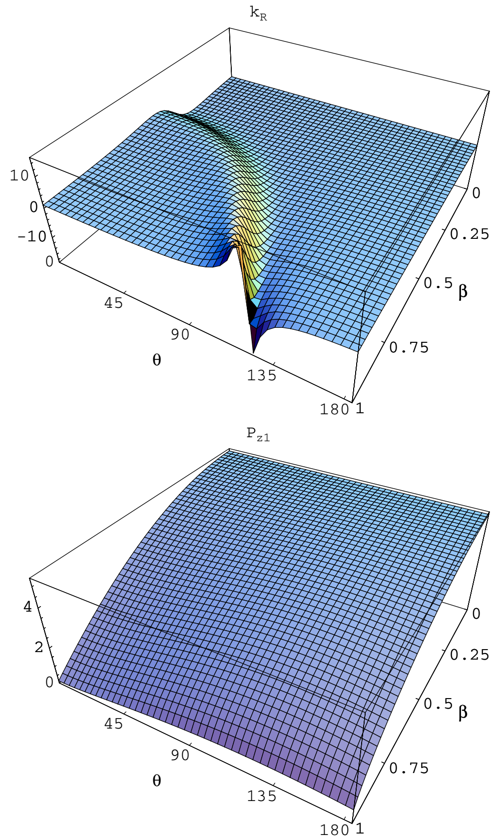

Figure 7. As figure 1 but with $\epsilon = -3 + i2\delta$ and $\mu = -2 + i\delta$.

and accompanying maximum values of k_I, are seen at large angles θ for $\delta = 0.1, 0.5$ and 1. As in figure 2, the positive-to-negative transition of k_R and the maximum of k_I are most noticeable for $\delta = 0.1$.

3.2. $\epsilon_R > 0$ *and* $\mu_R < 0$

The θ and β dependences of k_R, k_I, P_{z1} and P_{z2} are shown in figure 4 for $\epsilon = 3 + i2\delta$ and $\mu = -2 + i\delta$ with $\delta = 0.5$. As in figure 1, the PPV regime extends over much of the $\theta\beta$ plane, but a region of NPV behaviour—which extends over a larger area of the $\theta\beta$ plane than does the corresponding region in figure 1—is observed where θ and β have their largest values.

The k_R transition from positive to negative values is revealed in greater detail in figure 5 where k_R, k_I, P_{z1} and P_{z2} are plotted as functions of β for $\delta = 0.1, 0.5$ and 1. At $\theta = \pi/6, k_R > 0$ and PPV propagation is inferred for all values of $\beta \in (0, 1)$. However, for $\theta = 5\pi/6$, we see that $k_R < 0$ for all but the very smallest values of β. Furthermore, unlike the situation depicted in figures 1–3 for $\epsilon_R > 0$ and $\mu_R > 0$, here the transition from $k_R > 0$ to $k_R < 0$ is not accompanied by a local maximum in k_I. Indeed, as $\beta \to 1$, we see that the values of k_I become increasingly small whereas the values of $|k_R|$ become increasingly large.

The quantities k_R, k_I, P_{z1} and P_{z2} are considered as functions of θ in figure 6 for $\delta = 0.1, 0.5$ and 1. At $\beta = 0.3$, the real part (k_R) of the wavenumber k is positive at

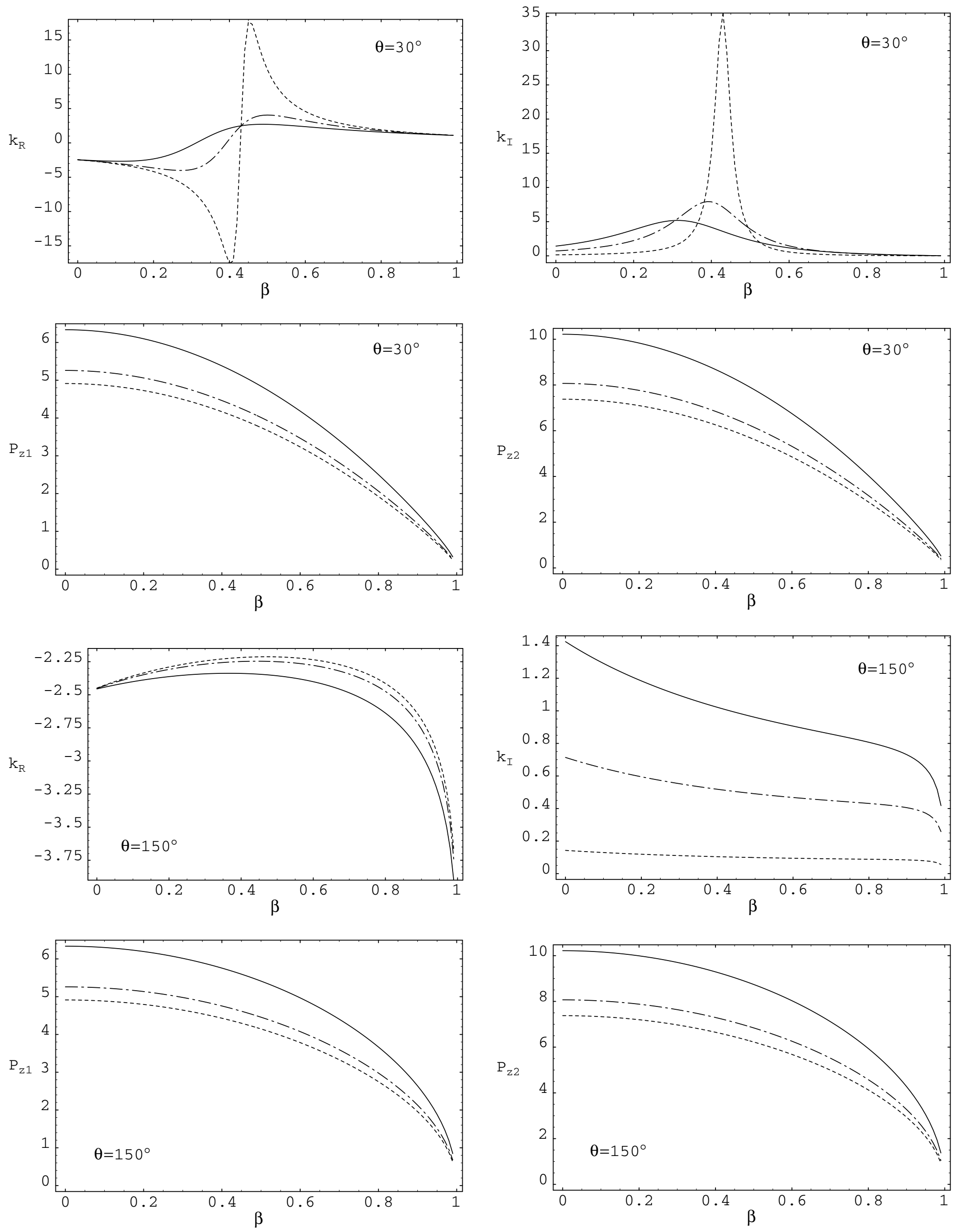

Figure 8. As figure 2 but with $\epsilon = -3 + i2\delta$ and $\mu = -2 + i\delta$.

low values of θ and becomes negative as θ increases beyond approximately $2\pi/3$. The transition from $k_R > 0$ to $k_R < 0$ coincides with a modest local maximum in k_I. At $\beta = 0.9$, the observed transition from $k_R > 0$ to $k_R < 0$ is rather more abrupt, as is the accompanying local maximum in k_I.

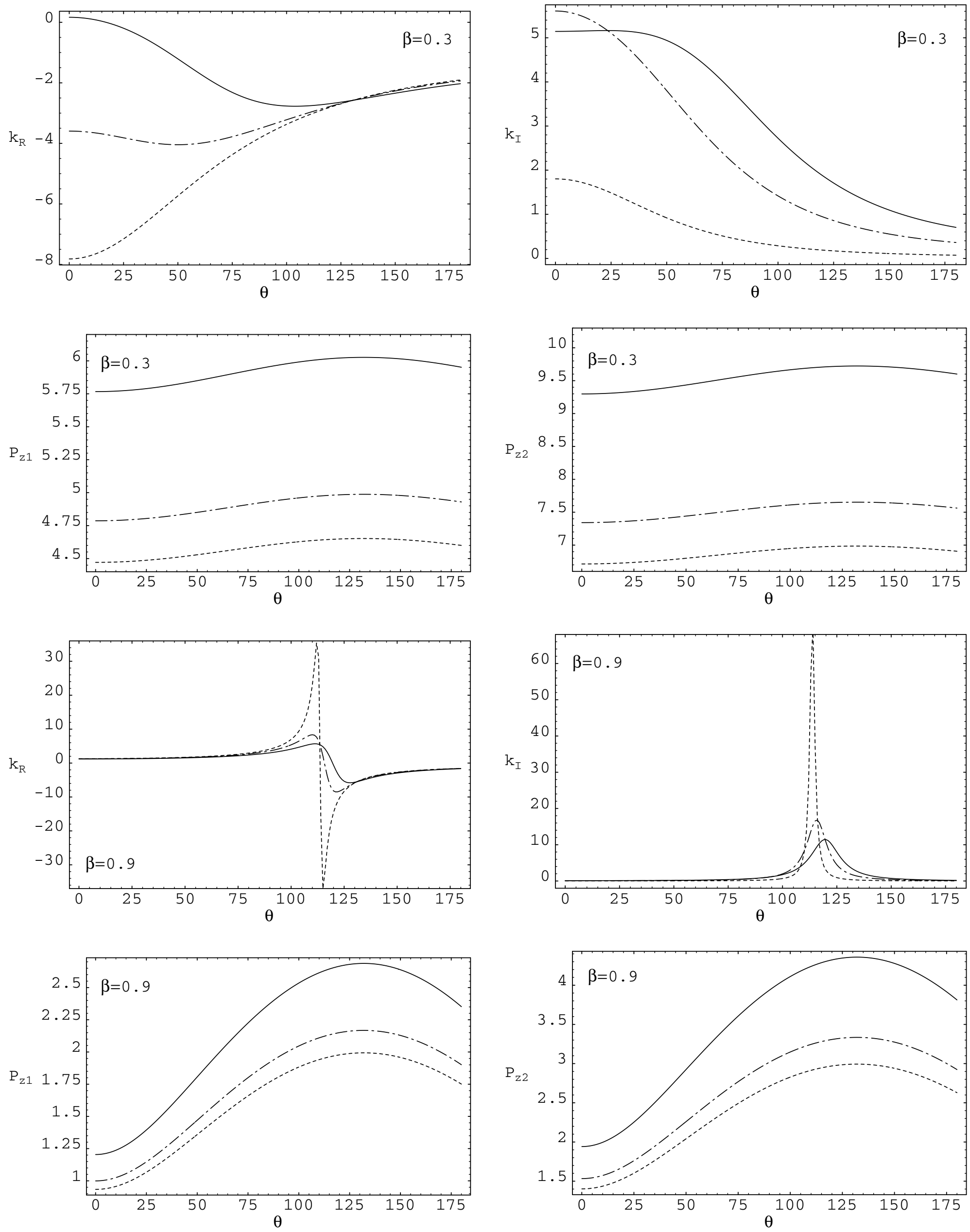

Figure 9. As figure 3 but with $\epsilon = -3 + i2\delta$ and $\mu = -2 + i\delta$.

3.3. $\epsilon_R < 0$ *and* $\mu_R < 0$

When both ϵ_R and μ_R are negative, we definitely expect to find NPV propagation in the co-moving reference frame (i.e. $\beta = 0$) [10]. The quantities k_R, k_I, P_{z1} and P_{z2} are plotted as functions of θ and β in figure 7 for $\epsilon = -3 + i2\delta$ and $\mu = -2 + i\delta$ with $\delta = 0.5$. The region of negative k_R (with k_I, P_{z1} and P_{z2} all positive) extends over much of the $\theta\beta$ plane. However, regions of positive k_R are also observed—at high values of β.

More detailed information is provided in figure 8 where k_R, k_I, P_{z1} and P_{z2} are plotted against β for $\delta = 0.1$, 0.5 and 1. At $\theta = \pi/6$, $k_R < 0$ for low values of β but becomes positive as β increases. The transition from $k_R < 0$ to $k_R > 0$ coincides with a local maximum in k_I, with the positive-to-negative transition of k_R and the maximum of k_I being particularly abrupt for $\delta = 0.1$. Thus, the NPV propagation which develops at low values of β (including $\beta = 0$) is replaced by PPV propagation at sufficiently large values of β.

Further insights may be gained by considering the plots of k_R, k_I, P_{z1} and P_{z2} as functions of θ in figure 9, for $\delta = 0.1$, 0.5 and 1. At $\beta = 0.3$, the NPV regime is observed to prevail for all values of $\theta \in (0, \pi)$, with the exception of very small values of θ for $\delta = 1$. On the other hand, at $\beta = 0.9$, $k_R > 0$ at low values of θ but undergoes a transition to become $k_R < 0$ as θ increases. The positive-to-negative transition of k_R is accompanied by a sharp local maximum in k_I, with the local maximum being particularly sharp for $\delta = 0.1$.

4. Conclusions

That isotropic homogeneous mediums characterized by $\epsilon_R < 0$ and $\mu_R < 0$ support NPV propagation has become firmly established in recent years [2, 10]. Furthermore, it was recently noted that NPV behaviour may develop if only one of ϵ_R or μ_R is less than zero [11]. It is demonstrated here that the $\{\epsilon_R, \mu_R\}$ regime giving rise to NPV behaviour may be extended considerably by considering planewave propagation in a uniformly moving reference frame.

In section 1 we asked the following question: Can a medium which is of the PPV type when viewed in a stationary reference frame be of the NPV type when viewed in a reference frame moving at constant velocity? 'Yes' is the answer. In particular,

(a) a stationary PPV medium with $\epsilon_R > 0$ and $\mu_R > 0$ may be viewed as a NPV medium provided it is moving at a sufficiently large uniform velocity;
(b) a stationary PPV medium with $\epsilon_R > 0$ and $\mu_R < 0$ (or $\epsilon_R < 0$ and $\mu_R > 0$) may be viewed as a NPV medium provided it is moving at a sufficiently large uniform velocity;
(c) a stationary NPV medium with $\epsilon_R < 0$ and $\mu_R < 0$ may be viewed as a PPV medium provided it is moving at a sufficiently large uniform velocity.

These findings have significant scientific and technogical implications for the realization of NPV propagation: to date, NPV propagation has been observed experimentally only in microwave metamaterials comprising conducting wire/ring inclusions, embedded periodically on printed circuit boards [3, 4]. It is demonstrated here that NPV propagation is achievable in *homogeneous* dielectric-magnetic mediums, when observed in a reference frame which is translated at a sufficiently high velocity. We expect these results to be significant for space telemetry, especially for remotely probing the surfaces of planets from space stations.

Acknowledgments

The authors thank an anonymous referee for suggesting improvements to the manuscript and drawing their attention to [18].

References

[1] Veselago V G 1968 The electrodynamics of substances with simultaneously negative values of ϵ and μ *Sov. Phys. Usp.* **10** 509–14

[2] Veselago V G 2003 Electrodynamics of media with simultaneously negative electric permittivity and magnetic permeability *Advances in Electromagnetics of Complex Media and Metamaterials* ed S Zoudhi, A Sihvola and M Arsalane (Dordrecht: Kluwer) pp 83–97

[3] Smith D R, Padilla W J, Vier D C, Nemat-Nasser S C and Schultz S 2000 Composite medium with simultaneously negative permeability and permittivity *Phys. Rev. Lett.* **84** 4184–7

[4] Shelby R A, Smith D R and Schultz S 2001 Experimental verification of a negative index of refraction *Science* **292** 77–9

[5] Grbic A and Eleftheriades G V 2002 Experimental verification of backward-wave radiation from a negative index metamaterial *J. Appl. Phys.* **92** 5930–5

[6] Houck A A, Brock J B and Chuang I L 2003 Experimental observations of a left-handed material that obeys Snell's law *Phys. Rev. Lett.* **90** 137401

[7] Ziolkowski R W and Heyman E 2001 Wave propagation in media having negative permittivity and permeability *Phys. Rev.* E **64** 056625

[8] Wang J and Lakhtakia A 2002 On reflection from a half-space with negative real permittivity and permeability *Microw. Opt. Technol. Lett.* **33** 465–7

[9] Felbacq D and Moreau A 2003 Direct evidence of negative refraction at media with negative ϵ and μ *J. Opt. A: Pure Appl. Opt.* **5** L9–L11

[10] Lakhtakia A, McCall M W and Weiglhofer W S 2003 Negative phase-velocity mediums *Introduction to Complex Mediums for Optics and Electromagnetics* ed W S Weiglhofer and A Lakhtakia (Bellingham, WA: SPIE)

[11] McCall M W, Lakhtakia A and Weiglhofer W S 2002 The negative index of refraction demystified *Eur. J. Phys.* **23** 353–9

[12] Hu L and Chui S T 2002 Characteristics of electromagnetic wave propagation in uniaxially anisotropic left-handed materials *Phys. Rev.* B **66** 085108

[13] Kärkkäinen M K 2003 Numerical study of wave propagation in uniaxially anisotropic Lorentzian backward-wave slabs *Phys. Rev.* E **68** 026602

[14] Mackay T G and Lakhtakia A 2004 Plane waves with negative phase velocity in Faraday chiral mediums *Phys. Rev.* E **69** 026602

[15] Chen H C 1983 *Theory of Electromagnetic Waves* (New York: McGraw-Hill) chapter 8

[16] Pappas C H 1988 *Theory of Electromagnetic Wave Propagation* (New York: Dover) chapter 7

[17] Chawla B R and Unz H 1971 *Electromagnetic Waves in Moving Magneto-plasmas* (Lawrence, KS: University Press of Kansas)

[18] Hagedorn R 1964 *Introduction to Field Theory and Dispersion Relations* (Oxford: Pergamon) appendix 5